Anomalous dispersion analysis of inhibitor flexibility – a case study on H-89

Alexander Pflug, Kenneth A. Johnson, Richard A. Engh

Norwegian Structural Biology Centre, Department of Chemistry, University of Tromsø, N-9037 Tromsø, Norway

Abstract

H-89 is a kinase inhibitor developed in the 1980s, prior to the era of structure-based design of kinase targeting drugs and kinome-wide selectivity screens. It was developed and reported to be selective towards cAMP dependent protein kinase, also known as protein kinase A (PKA). Probably because of the lack of alternatives and not least because it is a simple molecule, allowing for economical synthesis, H-98 is still widely used as a PKA inhibitor in research. By current standards, the compound is still fairly potent, but its kinase selectivity profile renders it as a rather general AGC kinase inhibitor than as a solely PKA-targeting agent. With the work presented here we intend to evaluate details of H-89 binding, including its binding flexibility, using anomalous dispersion methods.

Introduction

Besides Fasudil, H-89 is one of the most prominent representatives of the 'H-series' kinase inhibitors, a set of ATP competitive compounds designed on the basis of isoquinoline sulfonamides [1, 2, 3] (Figure 1). While Fasudil received approval by the Japanese authorities in 1995 for the prevention of cerebral vasospasm in patients with subarachnoid hemorrhage, and was found potentially useful to enhance memory and improve the prognosis

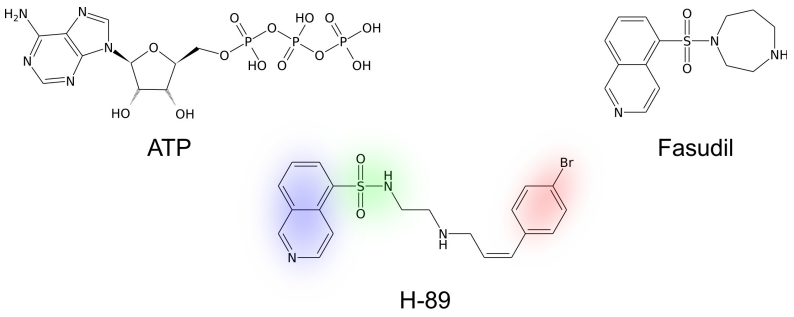

Figure 1: Molecule structures of Adenosine-5'-triphosphate (ATP), Fasudil and H-89. The isoquinoline portion of H-89 is highlighted in blue, the sulfonamide portion in green and the bromobenzene moiety in red.

of Alzheimers patients [4]; H-89's uses remain largely confined to academic research. This is based on the fact that PKA generally is regarded an 'antitarget', due to the ubiquitous and essential nature of cellular processes it regulates. However, especially for *in vitro* studies requiring absence of PKA activity or studies on the regulatory role of PKA itself, H-89 turned out to be very popular. And it still is used frequently, now in the context of recent studies that show H-89 to be rather a general AGC kinase inhibitor [5, 6]. H-89 found use outside the lab too. In drug development projects, its scaffold was derivatized in order to gain selectivity towards protein kinase B (PKB/Akt) [7, 8, 9]. PKB is structurally similar to PKA [10] and is an important drug target [11]. The co-crystal structure of PKA in complex with H-89 by Engh and co-workers (PDB ID: 1YDT) indicated that the bromobenzene moiety of the compound has a high degree of flexibility in the ATP pocket [12]. This aspect of H-89 binding we investigate here through anomalous dispersion techniques.

Experimental Procedures

Protein production, purification and crystallization

The full-length human catalytic subunit α of PKA (GenBank accession number NP_002721) was expressed in *Escherichia col*i BL21(DE3)-RIL cells (Stratagene) from a construct based on the vector pT7-7 in Studier- au-

toinduction medium [13]. The expression was carried out over a period of approximately 20 h at 24 °C. The subsequent procedures for protein purification followed previous protocols described by Engh and co-workers [12].

Co-crystallization of PKA and H-89 was carried out in hanging drops at 4 °C. The droplets, containing 10 mg/ml protein, 25 mM BisTris pH 7.0, 150 mM KCl, 1.5 mM octanoyl-N-methylglucamide, 1 mM protein kinase inhibitor peptide (5-24)-PKI (TTYADFIASGRTGRRNAIHD), and 5mM H-89 (added from a MeOH stock) were equilibrated against 12–20% (v/v) methanol. The crystals were harvested and flash-frozen using 30% 2-methyl-2,4-pentanediol as cryoprotectant.

Diffraction data collection and data processing

The diffraction of a frozen crystal was measured on beamline ID29 at the European Synchrotron Radiation Facility (ESRF, Grenoble, France). In order to obtain the anomalous signal from H-89's bromine, 241 images with an oscillation range of 0.9 ° were collected at a wavelength of 0.91969 Å. The subsequent processing of the data was carried out with the XDS package [14] and the CCP4 program suite [15]. The diffraction frames were integrated with XDS and the resulting intensities scaled with XSCALE, whereby Friedel pairs were not merged (option 'FRIEDEL'S_LAW=FALSE') (Table 1). The dataset was phased by molecular replacement with MOLREP [16] employing the coordinates of PDB entry 1YDT [12]. The structure factors were refined with REFMAC5 [17] (Table 2) and then merged with the columns 'DANO' and 'SIGDANO' of the unphased original *.mtz file using the program CAD. The resulting *.mtz file, containing both structure factors with phases and the anomalous signal of H-89's bromine, were employed to calculate anomalous difference Fourier maps with the program FFT [18]. Coordinate and molecular topology files for ligands were created with PRODRG [19].

Structure deposition

Coordinates and structure factors of the crystal structure were deposited in the Protein Data Bank (PDB) with the accession code xxxx.

Table 1: Selected columns from the XSCALE scaling statistics

Resolution Limit (Å)	Completeness of Data	I/Sigma	R-meas	Rmrgd-F	Anomal Corr	SigAno
35	0.0%	-99	-99.9%	-99.9%	0%	0
30	90.0%	65.84	2.6%	1.3%	35%	1.87
25	90.9%	32.47	2.0%	2.4%	3%	1.318
20	96.7%	62.23	2.4%	1.4%	75%	1.661
15	100.0%	56.57	2.5%	1.3%	57%	1.599
10	100.0%	59.68	2.1%	1.2%	47%	1.132
9	100.0%	54.8	2.2%	1.3%	53%	1.224
8	100.0%	53.6	2.4%	1.6%	42%	1.211
7	100.0%	50.58	2.7%	1.6%	44%	1.457
6	100.0%	46.3	2.8%	1.7%	36%	1.192
5	100.0%	46.07	2.8%	1.8%	22%	1.021
4	99.8%	46.41	2.9%	1.8%	15%	0.94
3.8	99.9%	43.37	3.2%	2.1%	13%	0.92
3.55	99.9%	40.27	3.5%	2.4%	4%	0.847
3.3	99.9%	35.2	4.0%	2.8%	8%	0.92
3.05	100.0%	30.36	4.9%	3.7%	10%	0.935
2.8	99.9%	23.71	6.5%	5.3%	9%	0.906
2.45	100.0%	16.07	10.1%	8.6%	6%	0.865
2.2	100.0%	10.88	15.5%	13.7%	3%	0.836
1.95	98.0%	5.68	29.7%	28.8%	3%	0.791
total	99.3%	19.08	6.9%	9.0%	6%	0.867

Table 2: Refinement and structure statistics of the PDB entry xxxx

Refinement	
R_{work} (%)	19.4
R_{free} (%)	24.2
Average B factor (A^2)	22.0
Number of protein atoms	3342
Number of solvent atoms (including ions)	165
Root mean square deviations	
Bond lengths (A^2)	0.011
Bond angles (°)	1.57
Ramachandran plot (%)	
Most favored	90.2
Additionally allowed	9.8
Generously allowed	0
Disallowed	0

Results

The anomalous signal in the collected dataset is rather weak (Table 1). The mean correlation factor between two random subsets ('Anomal corr') exceeds 30% and the mean anomalous difference in units of its estimated standard deviation (|F(+)-F(-)|/Sigma; 'SigAno') exceeds 1.0 only at resolutions coarser than ~5 Å. Although this is far below the requirements for a successful SAD phasing experiment [20], it was sufficient to unambiguously localize the positions of H-89's bromine moiety within the asymmetric unit (Figure 2).

The anomalous difference Fourier maps in Figure 2A display one strong feature in the asymmetric unit, which is dominant in the maps contoured at $3\,\sigma$ and $4\,\sigma$, and is unique in the map contoured at $5\,\sigma$. This peak corresponds to the localization of the bromine group of the compound H-89 which resides in the ATP pocket of PKA (Figure 2C). However, instead of one clear sphere of density, the anomalous signal appears spread out into two spheres, indicating two main localizations of the bromine moiety in the complex. This result correlates well with the unclear electron density (2mFo-DFc map) of H-89's bromobenzene group in the structure 1YDT (Figure 2B) [12], as well as the higher resolution H-89:PKA complex structure measured for this study (Figure 2C). In both cases it seems that H-89's bromobenzene

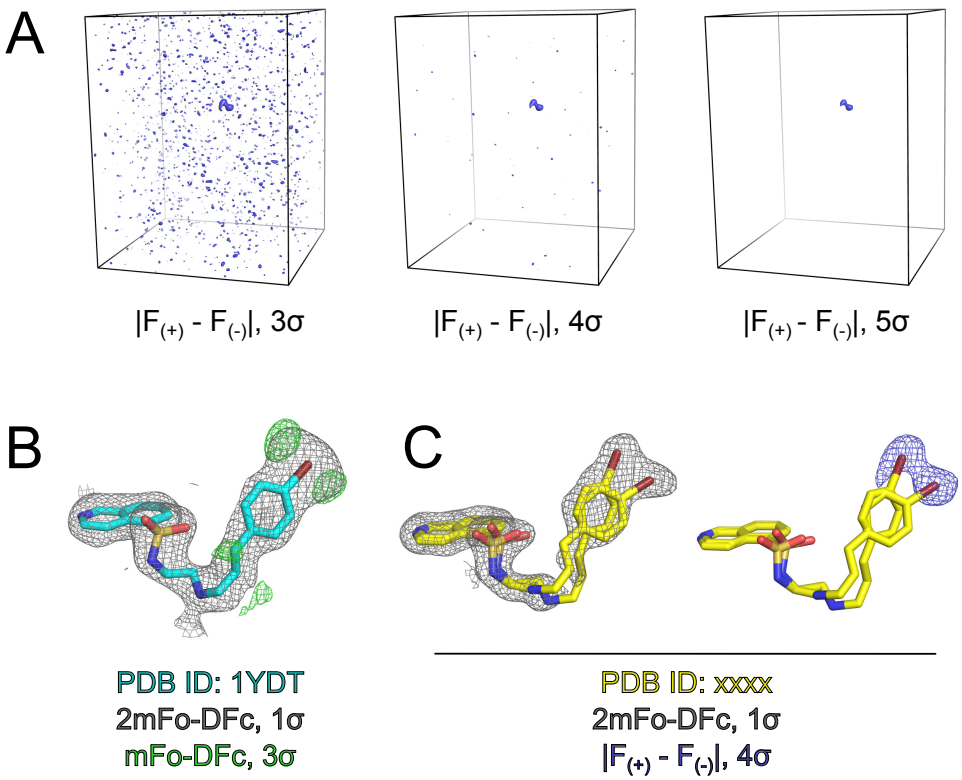

Figure 2: (A) Anomalous difference Fourier maps generated to cover all atoms of the asymmetric unit in PDB entry xxxx, contoured at σ levels 3, 4 and 5. (B) Electron density map (grey) and difference density map (green) carved around the compound H-89 in the PDB entry 1YDT (cyan) [12]. (C) Electron density map (grey) and anomalous difference density map (blue) carved around the compound H-89 with its two conformations in the PDB entry xxxx (yellow).

group has the freedom to rotate about an axis running perpendicular through its benzene ring. However, the electron density does not clearly define one or more preferred positions of the bromine moiety.

In contrast, the anomalous difference map draws a more clear picture with two spheres of density indicating two distinct positions of the bromine (Figure 2C). Based on this information H-89 was modeled in the structure xxxx with two alternative conformations. Starting the with the coordinates from the structure 1YDT, H-89 was split into two molecules with 50% occupancy each. By rotating the C3-N4 bond on the linker between the sulfonamide and bromobenzene group of H-89, the bromine moieties of the two alternative molecule conformations were placed in the positions indicated by the anomalous difference Fourier map. The coordinates were refined with default settings in REFMAC5 without positional restraints for the H-89 molecules resulting in the conformation presented in (Figure 2C). The bromobenzene moieties of the two conformers retained their positions, which is in agreement with the anomalous difference density. The isoquinoline head-groups of H-89 appear in generally identical positions, due to their fixation to the hinge region of the kinase domain. The linker linker regions that connect the aromatic moieties of H-89 show slight displacement depending on the positioning of the bromobenzene moieties in the respective confomer. This flexibility is in accord with the partial weak electron density (2mFo-DFc map) of this portion of H-89 in the structure xxxx (Figure 2C).

Discussion

The approval of using bromine containing molecules to use the anomalous signal to quickly identify bound ligand was employed extensively as a drug discovery business model [21, 22, 23], but published details of its utility are lacking. Here we show an application to identify a heterogeneous binding mode. Identification of partial occupancy is also required for weak binding ligands, so the approach is especially useful when used for low affinity fragments. Even in such difficult cases the incorporated anomalous scatterer would be detectable and allow for a clear identification of the fragments binding mode, provided the fragments bind in one or few unique positions. The electron density maps (2mFo-DFc) alone would not generally give enough evidence for the binding model with two alternative conformations.

The flexible binding mode of H-89 in the ATP pocket of PKA raises the

question if it is related to its promiscuous inhibition of AGC kinases [5, 6]. In order to develop H-89 towards a PKB inhibitor the linker between its aromatic moieties was rigidified, but the selectivity of the resulting compounds was not tested against a broader panel of AGC kinases [7, 8]. An interesting approach could be to modify H-89's linker to capture the two respective binding conformations and investigate potential changes in the compounds target selectivity pattern.

References

[1] Chijiwa T, Mishima A, Hagiwara M, Sano M, Hayashi K, et al. (1990) Inhibition of forskolin-induced neurite outgrowth and protein phosphorylation by a newly synthesized selective inhibitor of cyclic AMP-dependent protein kinase, n-[2-(p-bromocinnamylamino)ethyl]-5-isoquinolinesulfonamide (H-89), of PC12D pheochromocytoma cells. Journal of Biological Chemistry 265: 5267 –5272.

[2] Hidaka H, Inagaki M, Kawamoto S, Sasaki Y (1984) Isoquinolinesulfonamides, novel and potent inhibitors of cyclic nucleotide-dependent protein kinase and protein kinase c. Biochemistry 23: 5036–5041.

[3] Ono-Saito N, Niki I, Hidaka H (1999) H-series protein kinase inhibitors and potential clinical applications. Pharmacology & Therapeutics 82: 123–131.

[4] Huentelman MJ, Stephan DA, Talboom J, Corneveaux JJ, Reiman DM, et al. (2009) Peripheral delivery of a ROCK inhibitor improves learning and working memory. Behavioral neuroscience 123: 218–223.

[5] Davies SP, Reddy H, Caivano M, Cohen P (2000) Specificity and mechanism of action of some commonly used protein kinase inhibitors. The Biochemical Journal 351: 95–105.

[6] Lochner A, Moolman JA (2006) The many faces of h89: A review. Cardiovascular Drug Reviews 24: 261–274.

[7] Caldwell JJ, Davies TG, Donald A, McHardy T, Rowlands MG, et al. (2008) Identification of 4-(4-aminopiperidin-1-yl)-7H-pyrrolo[2,3-d]pyrimidines as selective inhibitors of protein kinase b through fragment elaboration. Journal of Medicinal Chemistry 51: 2147–2157.

[8] Collins I, Caldwell J, Fonseca T, Donald A, Bavetsias V, et al. (2006) Structure-based design of isoquinoline-5-sulfonamide inhibitors of protein kinase b. Bioorganic & Medicinal Chemistry 14: 1255–1273.

[9] Reuveni H, Livnah N, Geiger T, Klein S, Ohne O, et al. (2002) Toward a PKB inhibitor: modification of a selective PKA inhibitor by rational design. Biochemistry 41: 10304–10314.

[10] Gassel M, Breitenlechner CB, RÃŒger P, Jucknischke U, Schneider T, et al. (2003) Mutants of protein kinase a that mimic the ATP-binding site of protein kinase b (AKT). Journal of Molecular Biology 329: 1021–1034.

[11] Cheng JQ, Lindsley CW, Cheng GZ, Yang H, Nicosia SV (2005) The Akt/PKB pathway: molecular target for cancer drug discovery. Oncogene 24: 7482–7492.

[12] Engh RA, Girod A, Kinzel V, Huber R, Bossemeyer D (1996) Crystal structures of catalytic subunit of cAMP-dependent protein kinase in complex with isoquinolinesulfonyl protein kinase inhibitors h7, h8, and h89. structural implications for selectivity. The Journal of Biological Chemistry 271: 26157–26164.

[13] Studier FW (2005) Protein production by auto-induction in high density shaking cultures. Protein Expression and Purification 41: 207–234.

[14] Kabsch W (2010) XDS. Acta Crystallographica Section D Biological Crystallography 66: 125–132.

[15] Collaborative Computational Project N (1994) The CCP4 suite: programs for protein crystallography. Acta Crystallographica Section D Biological Crystallography 50: 760–763.

[16] Vagin A, Teplyakov A (1997) MOLREP : an automated program for molecular replacement. Journal of Applied Crystallography 30: 1022–1025.

[17] Murshudov GN, Vagin AA, Dodson EJ (1997) Refinement of macromolecular structures by the Maximum-Likelihood method. Acta Crystallographica Section D Biological Crystallography 53: 240–255.

[18] Ten Eyck LF (1973) Crystallographic fast fourier transforms. Acta Crystallographica Section A 29: 183–191.

[19] Schuttelkopf AW, van Aalten DMF (2004) PRODRG: a tool for high-throughput crystallography of protein-ligand complexes. Acta Crystallographica Section D, Biological Crystallography 60: 1355–1363.

[20] Dauter Z, Dauter M, Dodson E (2002) Jolly SAD. Acta Crystallographica Section D Biological Crystallography 58: 494–506.

[21] Antonysamy SS, Aubol B, Blaney J, Browner MF, Giannetti AM, et al. (2008) Fragment-based discovery of hepatitis c virus NS5b RNA polymerase inhibitors. Bioorganic & Medicinal Chemistry Letters 18: 2990–2995.

[22] Blaney J, Nienaber V, Burley SK (2006) Fragment-based lead discovery and optimization using X-Ray crystallography, computational chemistry, and high-throughput organic synthesis. In: Fragment-based Approaches in Drug Discovery, Wiley-VCH Verlag GmbH & Co. KGaA. pp. 215–248. URL `http://dx.doi.org/10.1002/3527608761.ch11`.

[23] Wolf E, De Angelis J, Khalil EM, Cole PA, Burley SK (2002) X-ray crystallographic studies of serotonin n-acetyltransferase catalysis and inhibition. Journal of Molecular Biology 317: 215–224.